Microstructure of Semicrystalline Poly(L-lactide)/Poly(4-vinylphenol) Blends Evaluated from SAXS Absolute Intensity Measurement

Hsin-Lung Chen,*,† Hsing-Huang Liu,† and J. S. Lin‡

Department of Chemical Engineering, National Tsing Hua University, Hsin-Chu, Taiwan 30013, R. O. C., and Solid State Division, Oak Ridge National Laboratory, Oak Ridge, Tennessee 37831

Received September 2, 1999; Revised Manuscript Received April 17, 2000

ABSTRACT: The semicrystalline morphology of melt-miscible poly(L-lactide) (PLLA)/poly(4-vinylphenol) (PVPh) blends was probed by small-angle X-ray scattering (SAXS) with the measurement of absolute intensity. Blending with PVPh enhanced the SAXS intensity associated with the lamellar stacks. This was attributed to the presence of PVPh in the interlamellar regions that enhanced the electron density contrast ($\Delta\eta$) between the crystalline and amorphous layers. The interlamellar morphology was quantitatively characterized by the magnitude of $\Delta\eta$ deduced from Strobl−Schneider's one-dimensional correlation function assuming the corresponding two-phase model. Good agreement between the measured $\Delta\eta$ and the values calculated by assuming a complete interlamellar incorporation indicated that nearly all PVPh was expelled into the interlamellar regions upon the crystallization of PLLA.

Introduction

Poly(L-lactide) (PLLA) is a crystalline biodegradable polyester with the T_g and the melting point of 60 and 180 °C, respectively. To achieve good property balances, PLLA had been blended with various commercial polymers to form miscible, partially miscible, and immiscible blends. The blending counterparts included ploy(ethylene oxide),[1−4] poly(DL-lactide),[5−9] polycaprolactone,[10−14] poly(vinyl acetate),[15,16] and polyacrylates.[17,18] The system of interest here is the blend of PLLA and amorphous poly(4-vinylphenol) (PVPh). Good miscibility is expected for these two polymers since the phenol moiety in PVPh is capable of forming hydrogen bonds with the carbonyl groups in aliphatic polyesters.[19]

PLLA/PVPh blend represents a crystalline/amorphous system wherein the crystallization usually involves two types of polymer transport, namely, diffusion of the crystalline component toward the crystal growth front and simultaneous segregation of the amorphous diluent away from the growth front. The morphological pattern is characterized by the distance over which the diluent is segregated, where the diluent may be expelled into the interlamellar (IL segregation), interfibrillar (IF segregation), or interspherulitic (IS segregation) regions.[20−22] These three morphological patterns represent the diluent dispersion from nanoscopic scale for IL segregation to micrometer scale for IS segregation. Different scales of dispersion may lead to different properties.

Small-angle X-ray scattering (SAXS) has been a powerful tool for probing the detailed microstructure of crystalline/amorphous blends. The morphological parameters in the lamellar level such as the long period (L), crystal thickness (l_c), and amorphous layer thickness (l_a) can be deduced from the one-dimensional correlation function or the interphase distribution function. Close examination on the composition variation of l_a may reveal the existence of IL segregation.[23−25] The volume fraction of lamellar stacks (ϕ_s) given by the ratio of bulk crystallinity (ϕ_c) to the crystallinity within the lamellar stacks (ϕ_{cs}), i.e., $\phi_s = \phi_c/\phi_{cs}$, could serve as a measure for the extent of IL segregation.[26,27] When the absolute scattering intensity is available, the perturbation of intensity upon blending may also be connected with the microstructure of crystalline/amorphous blends.

In the present study, we probe the morphological structure of semicrystalline PLLA/PVPh blends by means of SAXS with the measurement of absolute scattering intensity. It will be seen that PLLA/PVPh represents one of the few systems for which the effect of IL segregation on the scattering behavior can be directly demonstrated from the drastic change of scattering intensity with composition. In addition, with the absolute intensity, the electron density contrast between the crystalline and amorphous layers in the lamellar stacks can be evaluated very conveniently from the simple geometric analysis of the correlation function proposed by Strobl and Schneider.[28] The measured electron density contrast will be compared with the values calculated by assuming complete IL segregation to reveal the extent of IL segregation in semicrystalline PLLA/PVPh blends.

Experimental Section

Materials and Sample Preparation. PLLA with M_n = 82 000 and M_w = 153 000 was acquired from Sigma, and PVPh with M_n = 13 000 and M_w = 25 000 was obtained from Polysciences Inc. Blendings of PLLA and PVPh were carried out by solution casting using *N*,*N*-dimethylformamide (DMF) as the cosolvent.

Specimens for SAXS study were ca. 0.3 mm thick and were prepared by pressing the blends between two pieces of Teflon films on a Linkam HFS91 hot stage at 190 ± 0.2 °C for 5 min, followed by quickly transferring the samples into an oven equilibrated at the desired crystallization temperatures (T_c = 125 and 140 °C). The crystallizations were allowed to proceed for 48 h.

Bulk Crystallinity Measurements. Bulk crystallinities (ϕ_c) of semicrystalline PLLA/PVPh were calculated from the enthalpy of melting. The enthalpy of melting was measured by a TA Instrument 2000 differential scanning calorimeter (DSC). Bulk crystallinities were calculated by taking 93.1 J/g as the enthalpy of melting of 100% crystalline PLLA.[29]

† National Tsing Hua University.
‡ Oak Ridge National Laboratory.
* To whom correspondence should be addressed.

10.1021/ma991504o CCC: $19.00
Published on Web 06/01/2000

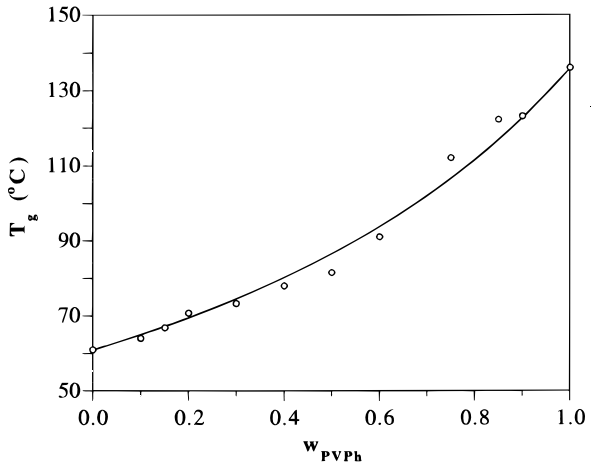

Figure 1. Composition variation of T_g of PLLA/PVPh blends quenched from 190 °C.

SAXS Measurement. SAXS experiments were performed at room temperature on the Oak Ridge National Laboratory (ORNL) 10 m SAXS instrument, with a sample-to-detector distance of 5 and 2 m using Cu Kα radiation ($\lambda = 1.54$ Å) and a 20×20 cm^2 two-dimensional position-sensitive detector with each virtual cell element of about 3 mm apart. The scattering intensity was stored in a 64×64 data array. Corrections were made for instrumental backgrounds, dark current due to cosmic radiation and electronic noises, and detector nonuniformity and efficiency (via an ^{55}Fe radioactive standard which emits γ-rays isotropically) on a cell-by-cell basis. The data were radially (azimuthually) averaged in the q range 0.1 nm^{-1} < q < 2.5 nm^{-1} ($q = 4\pi/\lambda \sin(\theta/2)$, where λ is the X-ray wavelength and θ is the scattering angle) and converted to an absolute differential scattering cross section by means of a precalibrated secondary standard.[30]

Results and Discussion

Figure 1 displays the composition variation of T_g of PLLA/PVPh quenched from 190 °C. Wide-angle X-ray diffraction indicated that the melt quenched blends were amorphous. A single composition-dependent T_g is identified over the entire composition range, indicating these two polymers are miscible in the melt. The phase behavior of PLLA/PVPh had also been studied by Zhang et al.[31] These two polymers were found to be partially miscible as the T_g did not exhibit a monotonic composition dependence. The conflict is presumably due to the higher molecular weight of PVPh (MW = 30 000) used in Zhang's study compared with that (MW = 13 000) used here or the different solvents (DMF vs THF) used in the blend preparation.

Because crystallization was extremely slow in the blends containing less than 80 wt % PLLA, we primarily focus on the morphological structure of the compositions with no more than 20 wt % PVPh. Figure 2 shows the Lorentz-corrected SAXS profiles of PLLA/PVPh crystallized at 125 and 140 °C. A second-order peak near 0.6 nm^{-1} can be roughly identified, indicating a fairly well lamellar stacking in the samples. Neat PLLA exhibits a very weak scattering peak due to low electron density contrast ($\Delta\eta = \eta_c - \eta_a$) between the crystalline and amorphous layers. The $\Delta\eta$ of neat PLLA calculated from the invariant (to be demonstrated later) is 0.015 mol/cm^3. The scattering intensity grows significantly upon blending for both T_c's. Because the electron density of PVPh (0.6268 mol/cm^3) is lower than that of amorphous PLLA (0.6608 mol/cm^3), the enhancement in scattering intensity is attributed to the incorporation of PVPh in the IL regions, as this would enhance the electron density contrast between the crystalline and amorphous layers. The SAXS profiles in Figure 2 provide straightforward evidence for the IL segregation of PVPh.

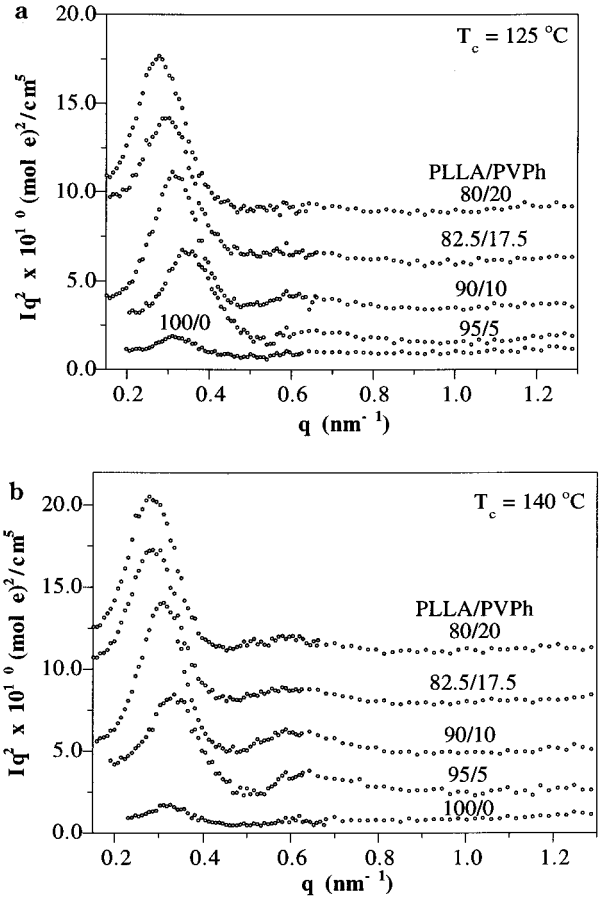

Figure 2. Lorentz-corrected SAXS profiles of PLLA/PVPh crystallized at (a) 125 and (b) 140 °C. The scattering intensity (I) is in units of (mol e)^2/cm^3. The scattering curves of the blends are displaced vertically for clear comparison.

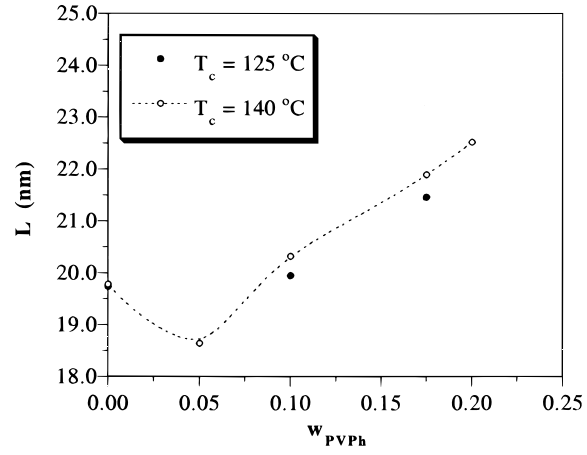

Figure 3. Composition variation of long period of semicrystalline PLLA/PVPh. The experimental error is about 5%.

The weight-average long period associated with the lamellar stacks can be calculated from the peak maximum using Bragg's equation, $L = 2\pi/q_{max}$. Figure 3 displays the composition variation of the long period. For both T_c's, the long period shows a minimum at $w_{PVPh} = 0.05$. Since the long period represents the sum of the crystal thickness and the amorphous layer thickness,

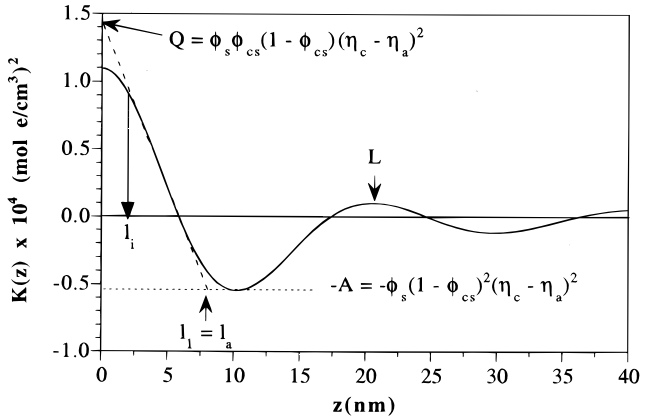

Figure 4. Representative plot of Strobl−Schneider's one-dimensional correlation function. Determinations of the lamellar layer thickness and the invariant assuming the corresponding two-phase model are demonstrated in the figure.

the one-dimensional correlation function was utilized to deconvolute the long period into the thickness of these two types of layers. The correlation function, $K(z)$, defined by Strobl and Schneider, adopts the following form:[28]

$$K(z) = \frac{1}{2\pi^2}\int_0^\infty Iq^2 \cos qz \, dq \qquad (1)$$

where I is the absolute intensity. $K(z)$ is different from the correlation function, $\gamma(z)$, defined by Vonk, where normalization by the invariant was introduced for $\gamma(z)$.[32,33] Figure 4 shows the representative plot of $K(z)$. Assuming the corresponding two-phase model, l_c and l_a can be estimated via simple geometric analysis of $K(z)$. The thickness of the thinner layers (l_1) is given by the intersection between the straight line extended from the self-correlation triangle and the baseline given by $-A$. The average thickness of the thicker layer is then given by $l_2 = L - l_1$. The assignment of l_1 and l_2 is governed by the magnitude of the crystallinity within the lamellar stacks (ϕ_{cs}). When $\phi_{cs} < 0.5$, the crystals contribute to the smaller thickness; then $l_1 = l_c$ and $l_2 = l_a$. The inverse is true for $\phi_{cs} > 0.5$. ϕ_{cs} is related to the bulk crystallinity, ϕ_c, by

$$\phi_c = \phi_s\phi_{cs} \qquad (2)$$

where ϕ_s is the volume fraction of lamellar stacks in the sample. Since $\phi_s \leq 1$, eq 2 prescribes that ϕ_c cannot be higher than ϕ_{cs}. As a result, the assignment of l_1 and l_2 would be rather straightforward for $\phi_c > 0.5$, because l_2 in this case must correspond to l_c and l_1 to l_a. Under the prescribed crystallization conditions, ϕ_c of all investigated PLLA/PVPh compositions lied above 55%; l_1 and l_2 were thus assigned as l_a and l_c, respectively.

Figure 5 plots l_c and l_a against the weight fraction of PVPh (w_{PVPh}). Like the long period, l_c reaches a minimum at $w_{PVPh} = 0.05$ for both T_c's. Dilution with 5 wt % of PVPh reduces the crystal thickness by ca. 5 nm. The crystal thickness however increases slightly (≤2 nm) with further addition of PVPh. The slight rise of l_c can be associated with the assumption of corresponding two-phase model in deriving l_c and l_a from $K(z)$, where the thickness of the crystal−amorphous interphase (l_i) is "included" into the values of l_c and l_a. The interphase thickness can be estimated from the deviation from the self-correlation triangle near $z = 0$ (Figure 4). The

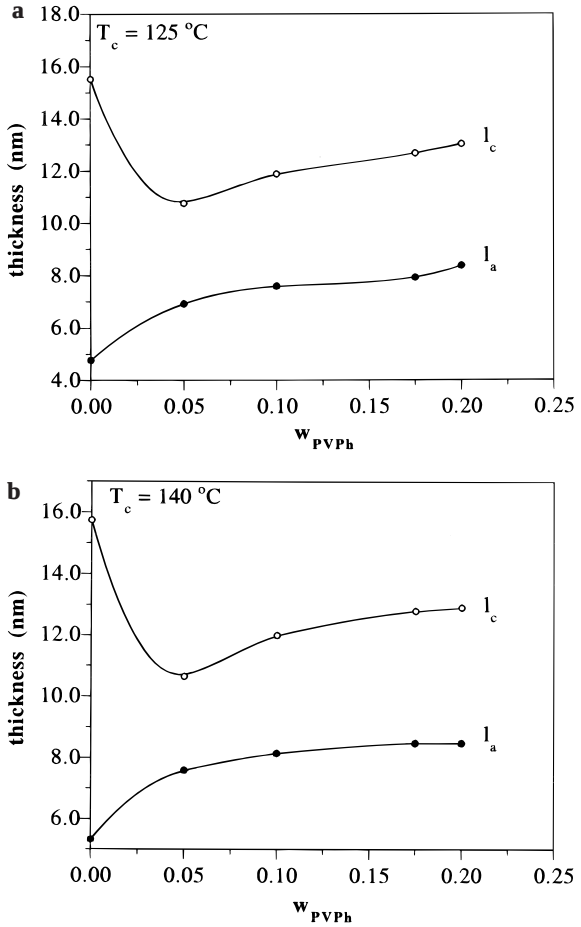

Figure 5. Composition variations of l_c and l_a of PLLA/PVPh crystallized at (a) 125 and (b) 140 °C.

Table 1. Thickness of Crystal−Amorphous Interphase (l_i) Estimated from $K(z)$

w_{PVPh}	T_c = 125 °C l_i (nm)	T_c = 140 °C l_i (nm)
0.00	0.66	1.02
0.05	1.86	1.90
0.10	2.35	2.40
0.125	2.45	2.87
0.2	2.82	3.31

values of l_i thus obtained are tabulated in Table 1. The interphase thickness appears to increase with PVPh composition, so the inclusion of l_i into l_c may be responsible for the observed rise of crystal thickness as $w_{PVPh} > 0.05$. Variation of l_a with PVPh composition is also displayed in Figure 5. The amorphous layer thickness increases monotonically with PVPh composition, where the increase is larger than the magnitude of l_i. Therefore, the swelling of l_a is attributed to the incorporation of PVPh in the IL regions, which is consistent with the enhancement of scattering intensity observed in Figure 2.

It is noted that the values of l_a and l_c determined from $K(z)$ could face a large uncertainty because the broad lamellar size distribution could shift the position of the baseline ($-A$).[28] On the other hand, the electron density contrast, $\Delta\eta$, can be determined from $K(z)$ with better confidence in that $\Delta\eta$ is much less sensitive to the perturbation of baseline position for the samples with intermediate crystallinity ($0.3 < \phi_{cs} < 0.7$). As shown in Figure 4, the invariant (Q) of the corresponding two-phase model is obtained by extrapolation from the self-

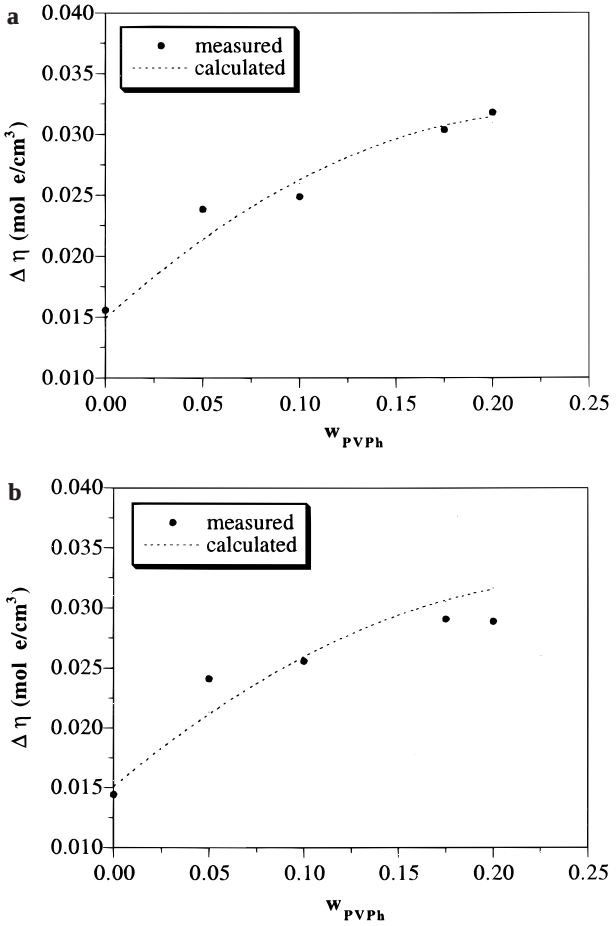

Figure 6. Comparison between the measured $\Delta\eta$ and the values calculated by assuming a complete interlamellar segregation (represented by the dashed line) for (a) $T_c = 125$ °C and (b) $T_c = 140$ °C.

correlation triangle to $z = 0$.[28] The invariant is related to the electron density contrast by

$$Q = \phi_s\phi_{cs}(1 - \phi_{cs})\Delta\eta^2 \quad (3)$$

where ϕ_{cs} is the crystallinity within the lamellar stacks given by

$$\phi_{cs} = 1 - \frac{A}{A + Q} \quad (4)$$

and ϕ_s is obtained by ϕ_c/ϕ_{cs} (ϕ_c was measured from the enthalpy of melting). $\Delta\eta$ can be calculated by eq 3 with the knowledge of Q, ϕ_{cs}, and ϕ_s. Figure 6 plots $\Delta\eta$ as a function of w_{PVPh}. The value of $\Delta\eta$ obtained for neat PLLA is 0.0155 mol/cm^3 for $T_c = 125$ °C and 0.0145 mol/cm^3 for $T_c = 140$ °C; the average value of 0.0150 mol/cm^3 is hence considered in the following analysis. The electron density of amorphous PLLA is 0.6608 mol/cm^3 calculated from the density of 1.2521 g/cm^3 measured by the density gradient column. Taking $\Delta\eta = 0.0150$ mol/cm^3, the electron density of crystalline PLLA is found to be 0.6758 mol/cm^3, which would correspond to the crystalline density of 1.280 g/cm^3. This value agrees very well with the crystalline density of 1.285 g/cm^3 reported by Miyata et al.[34]

For both T_c's, $\Delta\eta$ grows monotonically with PVPh composition, which affirmatively establish the incorporation of PVPh in the IL regions. The electron density contrast of the IL amorphous region can be expressed as

$$\Delta\eta = \phi_{PVPh}{}^{IL}\Delta\eta_{PVPh} + (1 - \phi_{PVPh}{}^{IL})\Delta\eta_{PLLA} \quad (5)$$

where $\phi_{PVPh}{}^{IL}$ is the volume fraction of PVPh in the IL regions, $\Delta\eta_{PVPh} = 0.0489$ mol/cm^3 is the electron density contrast between crystalline PLLA and PVPh, and $\Delta\eta_{PLLA} = 0.0150$ mol/cm^3 is the contrast between crystalline and amorphous PLLA. Assuming a complete IL segregation of PVPh, the weight fraction of PVPh in the IL regions can be easily obtained by

$$w_{PVPh}{}^{IL} = \frac{w_{PVPh}{}^{0}}{1 - w_c} \quad (6)$$

where $w_{PVPh}{}^0$ is the overall weight fraction of PVPh in the blend and w_c is the weight fraction of PLLA crystals. After converting $w_{PVPh}{}^{IL}$ into the volume fraction ($\phi_{PVPh}{}^{IL}$), the expected electron density contrast for a full IL segregation can be calculated by eq 5. Figure 6 compares the calculated $\Delta\eta$ (represented by the dashed line) with the measured values. Good agreement between the measured and calculated values is found over the composition range investigated, showing that nearly all PVPh was segregated into the IL regions during the crystallization of PLLA at both T_c's.

Conclusions

PLLA and PVPh formed miscible blends in the melt over the entire composition range. As semicrystalline PLLA exhibited a very weak SAXS peak and slight incorporation of PVPh into the IL regions would enhance the scattering intensity drastically, PLLA/PVPh represents one of the few systems for which the effect of IL morphology on the scattering behavior can be clearly revealed. In the semicrystalline state, the amorphous layers in the lamellar stacks were swollen upon blending, indicating that crystallization of PLLA preferentially expelled PVPh into the IL regions. The electron density contrast calculated from the absolute invariant also supported the IL morphology. Comparing the measured $\Delta\eta$ with the values calculated by assuming complete IL segregation indicated that nearly all PVPh was present in the IL regions upon crystallization of PLLA.

Acknowledgment. This work is supported by the National Science Council, R.O.C., under Grant NSC 89-2216-E-007-014 and also in part by the Division of Materials Sciences, U.S. Department of Energy, under Contract DE-AC05-96OR22464 with Lockheed Martin Energy Research, Corp.

References and Notes

(1) Nakafuku, C.; Sakoda, M. *Polym. J.* **1993**, *25*, 909.
(2) Nakafuku, C. *Polym. J.* **1994**, *26*, 680.
(3) Nakafuku, C. *Polym. J.* **1996**, *28*, 568.
(4) Nijenhuis, A. J.; Colstee, E.; Grijpma, D. W.; Pennings, A. J. *Polymer* **1996**, *37*, 5849.
(5) Jorda, R.; Wilkes, G. L. *Polym. Bull.* **1988**, *20*, 479.
(6) Tsuji, H.; Ikada, Y. *Macromolecules* **1992**, *25*, 5719.
(7) Tsuji, H.; Ikada, Y. *J. Appl. Polym. Sci.* **1995**, *58*, 1793.
(8) Tsuji, H.; Ikada, Y. J. *Polymer* **1996**, *37*, 595.
(9) Tsuji, H.; Ikada, Y. *J. Appl. Polym. Sci.* **1997**, *63*, 855.
(10) Grijma, D. W.; Van Hofslot, R. D. A.; Super, H.; Nijenhuis, A. J.; Pennings, A. *Polym. Eng. Sci.* **1994**, *34*, 1674.
(11) Hiljanen-Vainiu, M.; Varpomaa, P.; Seppla, J.; Tormala, P. *Macromol. Chem. Phys.* **1996**, *197*, 1503.

(12) Yang, J.-M.; Chen, H.-L.; You, J.-W.; Hwang, J. C. *Polym. J.* **1997**, *29*, 657.
(13) Tsuji, H.; Ikada, Y. *J. Appl. Polym. Sci.* **1998**, *67*, 405.
(14) Tsuji, H.; Mizuno, A.; Ikada, Y. *J. Appl. Polym. Sci.* **1998**, *70*, 2259.
(15) Gajria, A. M.; Dave', V.; Gross, R. A.; McCarthy, S. P. *Polymer* **1996**, *37*, 437.
(16) Ogata, N.; Jimenez, T. *J. Polym. Sci., Polym. Phys. Ed.* **1997**, *35*, 389.
(17) Eguiburu, J. L.; Iruin, J. J.; Fernandez-Berridi, M. J.; Roman, J. S. *Polymer* **1998**, *39*, 6891.
(18) Wu, G.-M.; Lee, J.-C.; Chen, H.-L.; Lin, T.-L. *Polymer*, in press.
(19) Landry, M. R.; Massa, D. J.; Landry, C. J. T.; Teegarden, D. M.; Colby, R. H.; Long, T. E.; Henrichs, P. M. *J. Appl. Polym. Sci.* **1994**, *54*, 991.
(20) Stein, R. S.; Khambatta, F. B.; Warner, F. P.; Russell, T.; Escala, A.; Balizer, E. *J. Polym. Sci., Polym. Symp.* **1978**, *63*, 313.
(21) Russell, T. P.; Ito, H.; Wignall, G. D. *Macromolecules* **1988**, *21*, 1703.
(22) Defieuw, G.; Groeninckx, G.; Renaers, H. *Polymer* **1989**, *30*, 595.
(23) Wenig, W.; Karasz, F. E.; MacKnight, W. J. *J. Appl. Phys.* **1975**, *46*, 4194.
(24) Khambatta, F. B.; Warner, F.; Rusell, T. P.; Stein, R. S. *J. Polym. Sci., Polym. Phys. Ed.* **1976**, *14*, 1391.
(25) Russell, T. P.; Stein, R. S. *J. Polym. Sci., Polym. Phys. Ed.* **1983**, *21*, 999.
(26) Chen, H.-L.; Wang, S.-F.; Lin, T.-L. *Macromolecules* **1998**, *31*, 8924.
(27) Chiu, H.-J.; Chen, H.-L.; Lin, T.-L.; Lin, J. S. *Macromolecules* **1999**, *32*, 2, 4969.
(28) Strobl, G. R.; Schneider, M. *J. Polym. Sci., Polym. Phys. Ed.* **1980**, *18*, 1343.
(29) Fischer, E. W.; Sterzel, H. J.; Wegner, G. *Kolloid Z. Z. Polym.* **1973**, *251*, 980.
(30) Russell, T. P.; Lin, J. S.; Spooner, S.; Wignall, G. D. *J. Appl. Crystallogr.* **1988**, *21*, 629.
(31) Zhang, L.; Goh, S. H.; Lee, S. Y. *Polymer* **1998**, *39*, 4847.
(32) Kortleve, G.; Vonk, V. G. *Kolloid-Z.* **1967**, *220*, 19.
(33) Kortleve, G.; Vonk, V. G. *Kolloid-Z.* **1968**, *225*, 124.
(34) Miyata, T.; Masuko, T. *Polymer* **1997**, *38*, 4003.

MA991504O